Supplemental Material : Scalar activity induced phase separation and liquid-solid transition in Lennard-Jones system

(a)

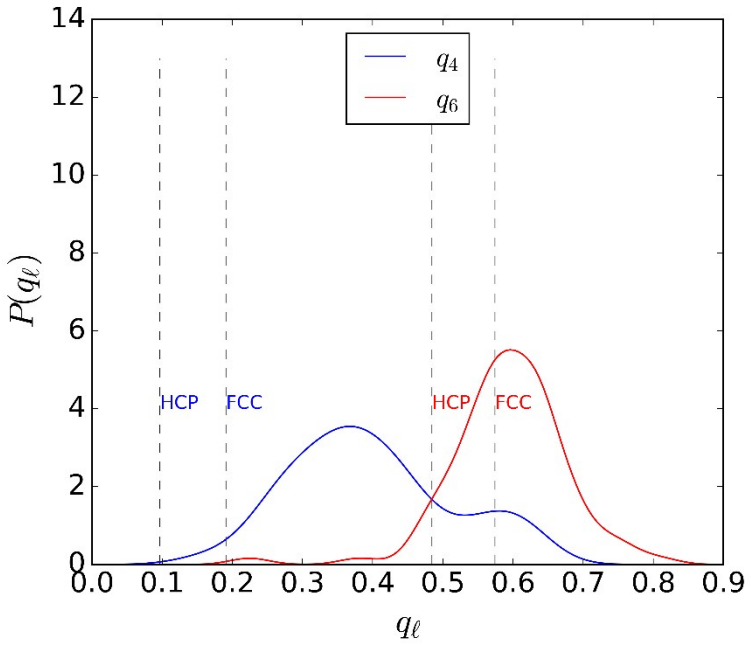

(b)

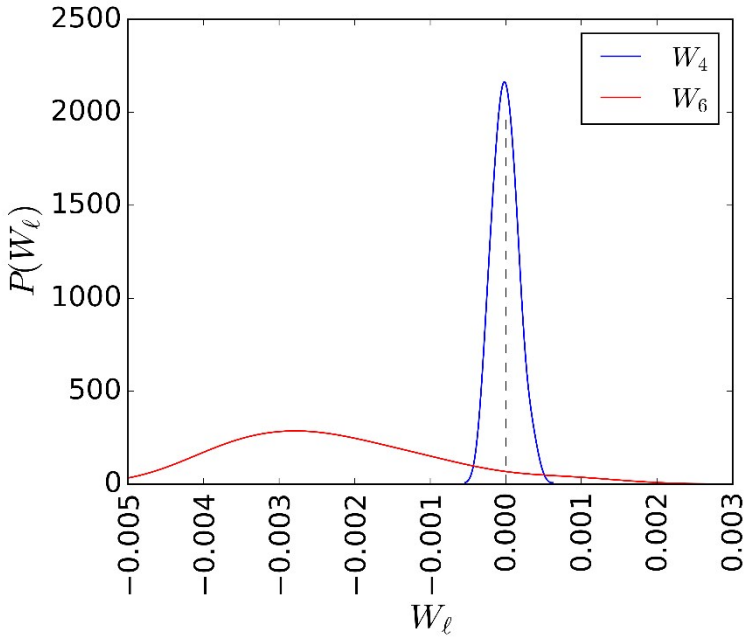

Figure SF1. (color online) Distributions of (a) q_4, q_6, (b) W_4, W_6, obtained only for hot particles, for the system with density $\rho^* = 0.1$ and N = 8000, at $T_h^* = 80$.

(a)

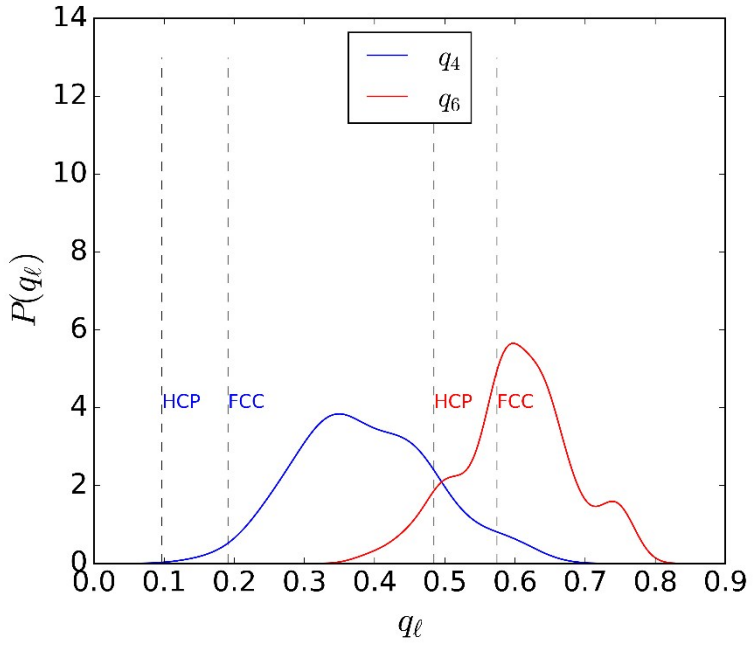

(b)

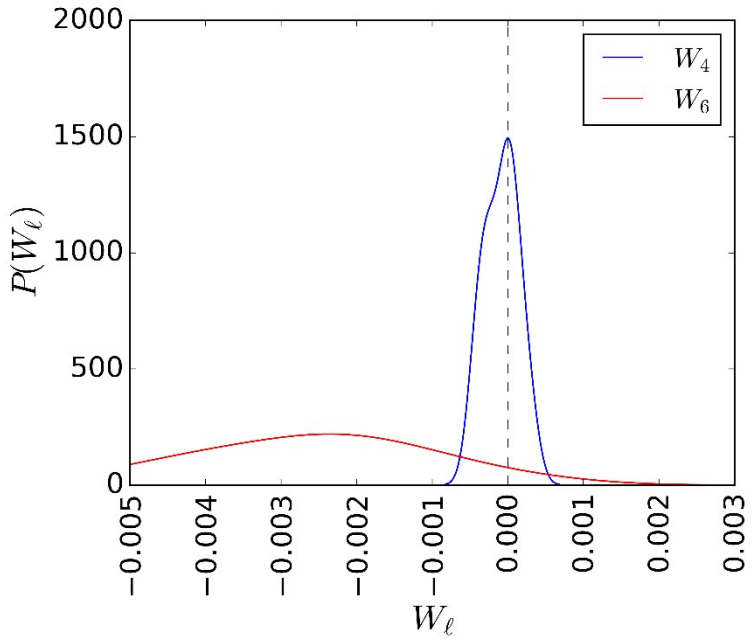

Figure SF2. (color online) Distributions of (a) q_4, q_6, (b) W_4, W_6, obtained only for hot particles, for the system with density $\rho^* = 0.2$ and N = 8000, at $T_h^* = 80$.

(a)

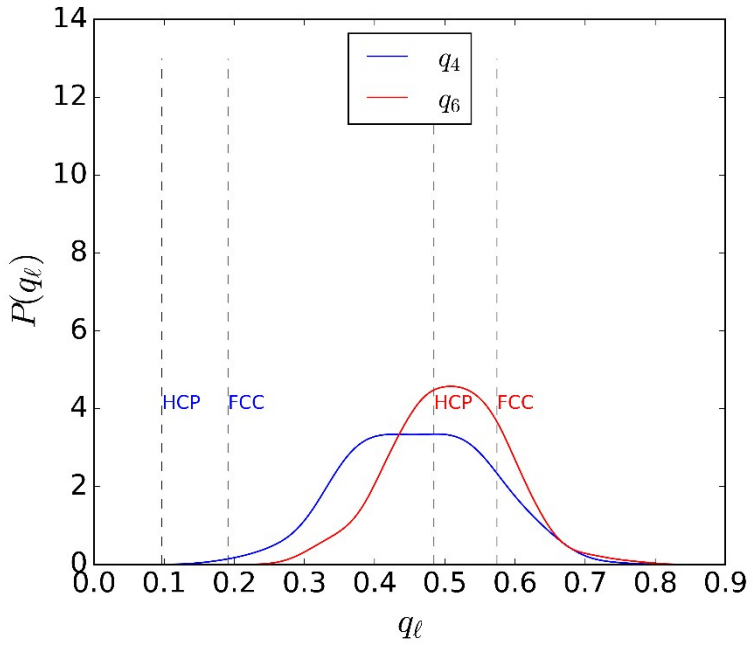

(b)

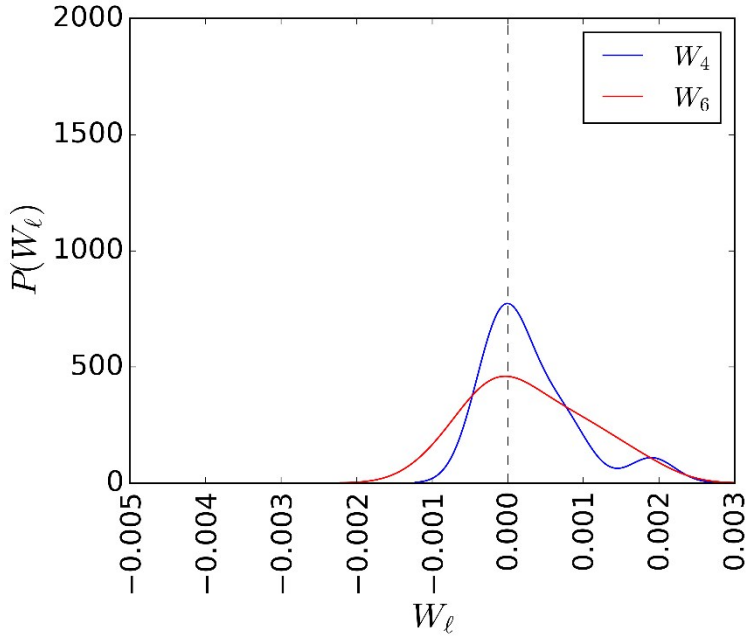

Figure SF3. (color online) Distributions of (a) q_4, q_6, (b) W_4, W_6, obtained only for hot particles, for the system with density $\rho^* = 0.5$ and N = 8000, at $T_h^* = 80$.

(a)

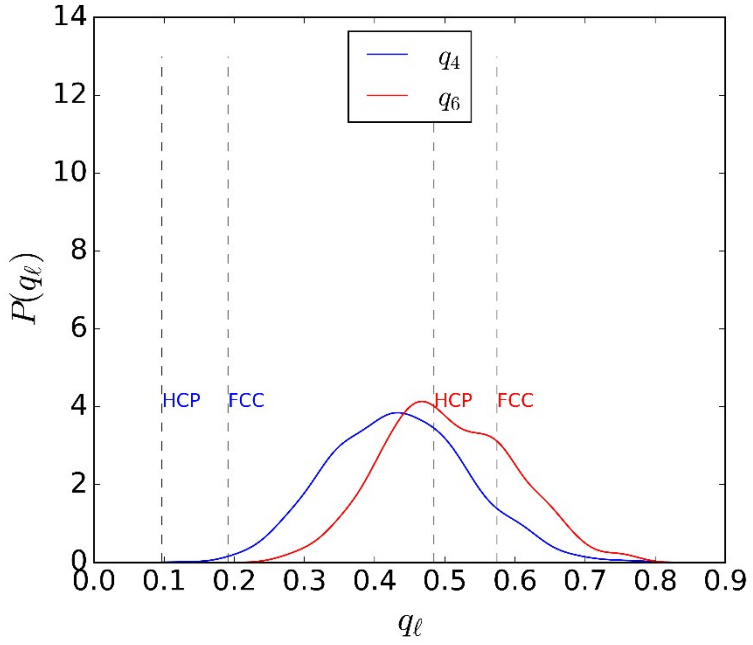

(b)

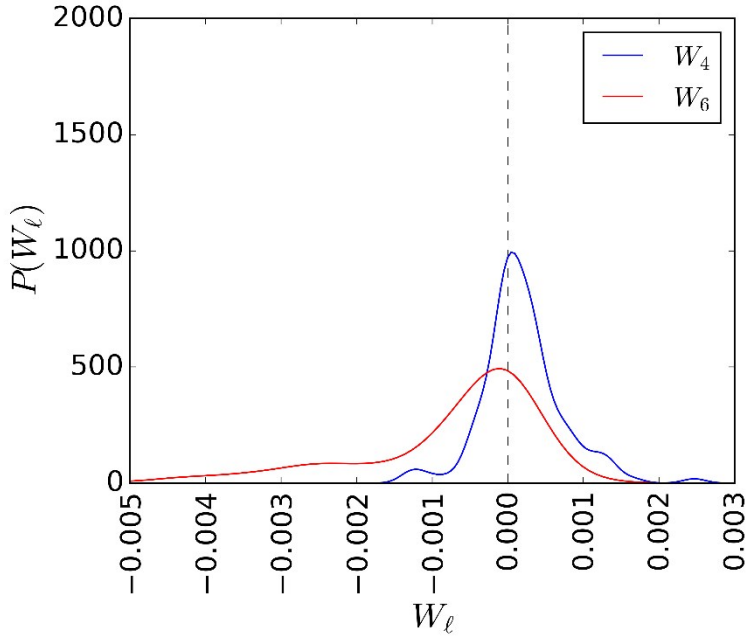

Figure SF4. (color online) Distributions of (a) q_4, q_6, (b) W_4, W_6, obtained only for hot particles, for the system with density $\rho^* = 0.8$ and N = 8000, at $T_h^* = 80$.

(a)

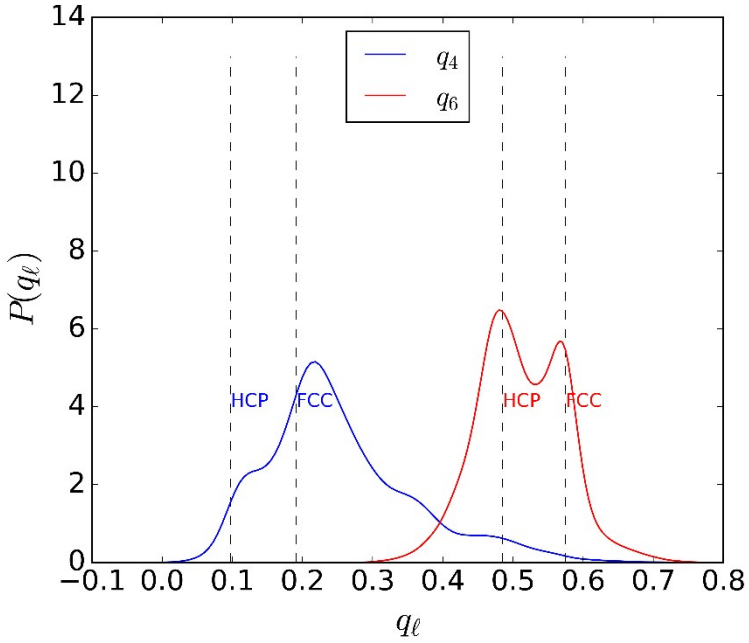

(c)

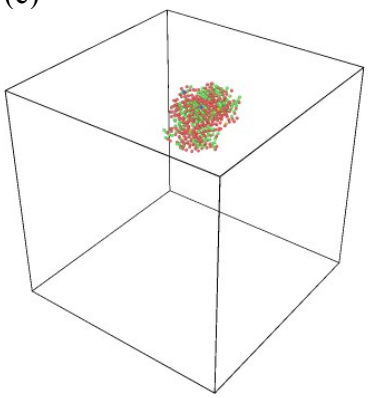

(b)

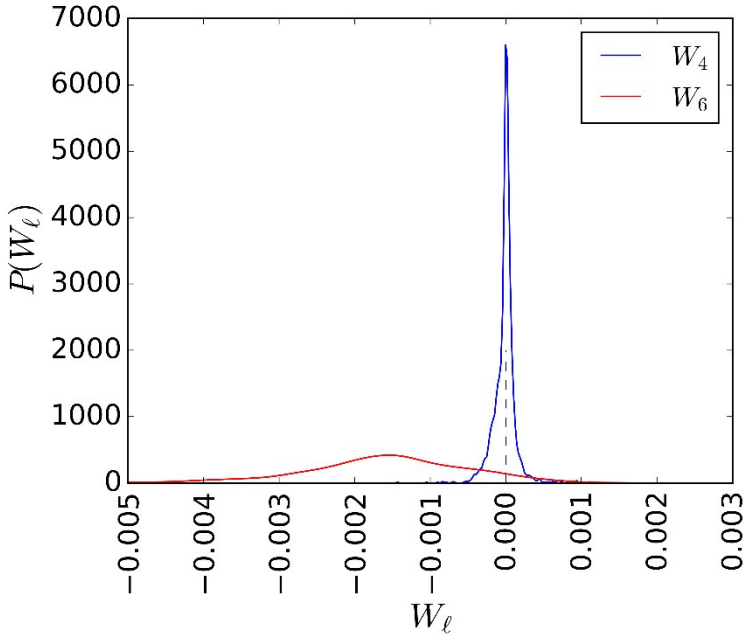

Figure SF5. (color online) System with $\rho^* = 0.1$: (a). From the distributions of q_4, q_6 indicating both FCC and HCP arrangement in the segregation. (b). The range of W_6 and W_4 also confirms the same (c). snaphot of the system with common neighbor analysis (CNA); green and red colors represent the FCC and HCP structures respectively. The snapshots and the CNA are performed using OVITO software.

(a)

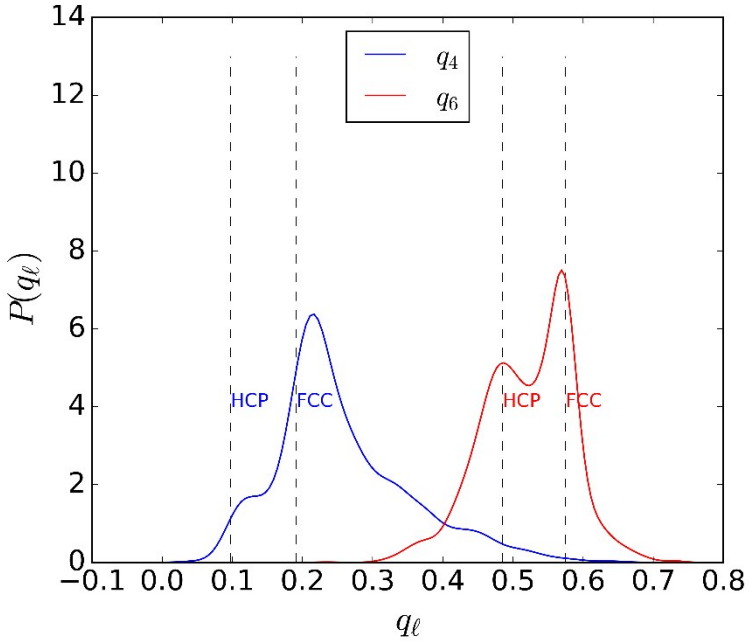

(c)

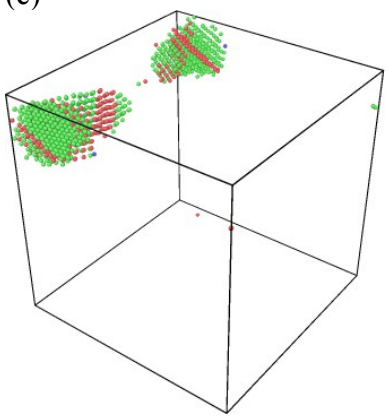

(b)

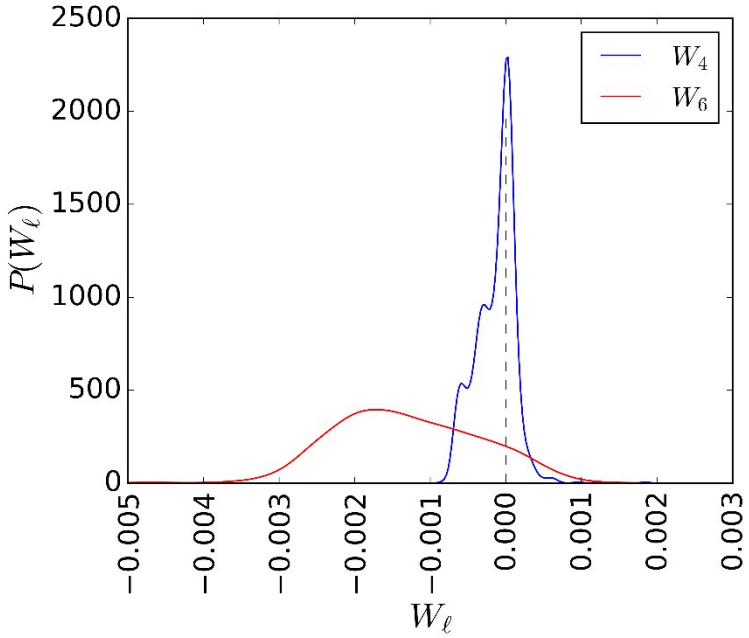

Figure SF6. (color online) Distributions of (a). q_4, q_6 and (b). W_4, W_6 parameters, at the density of $\rho^* = 0.2$. (c). snapshot of the system with CNA, green and red corresponds to FCC and HCP respectively.

(a)

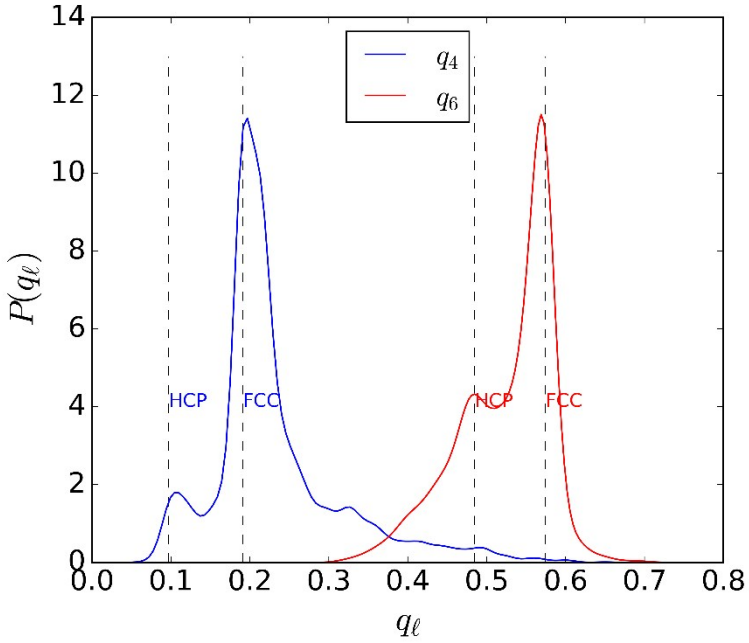

(c)

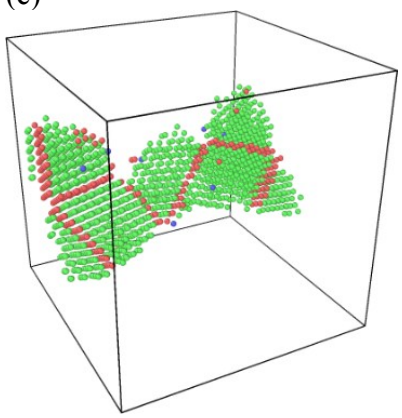

(b)

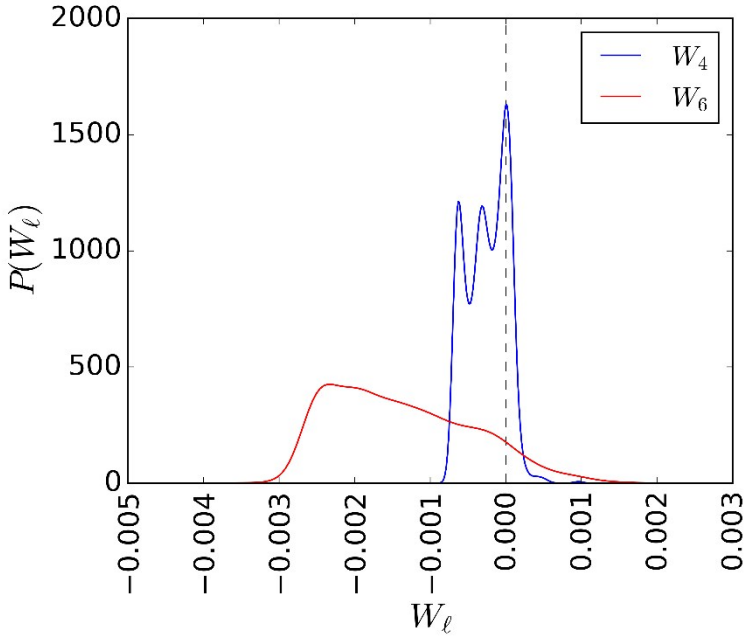

Figure SF7. (color online) Distributions of (a). q_4, q_6 and (b). W_4, W_6 parameters, at the density of $\rho^* = 0.5$. (c). system snapshot with CNA, green and red color denote the FCC and HCP arrangements respectively.

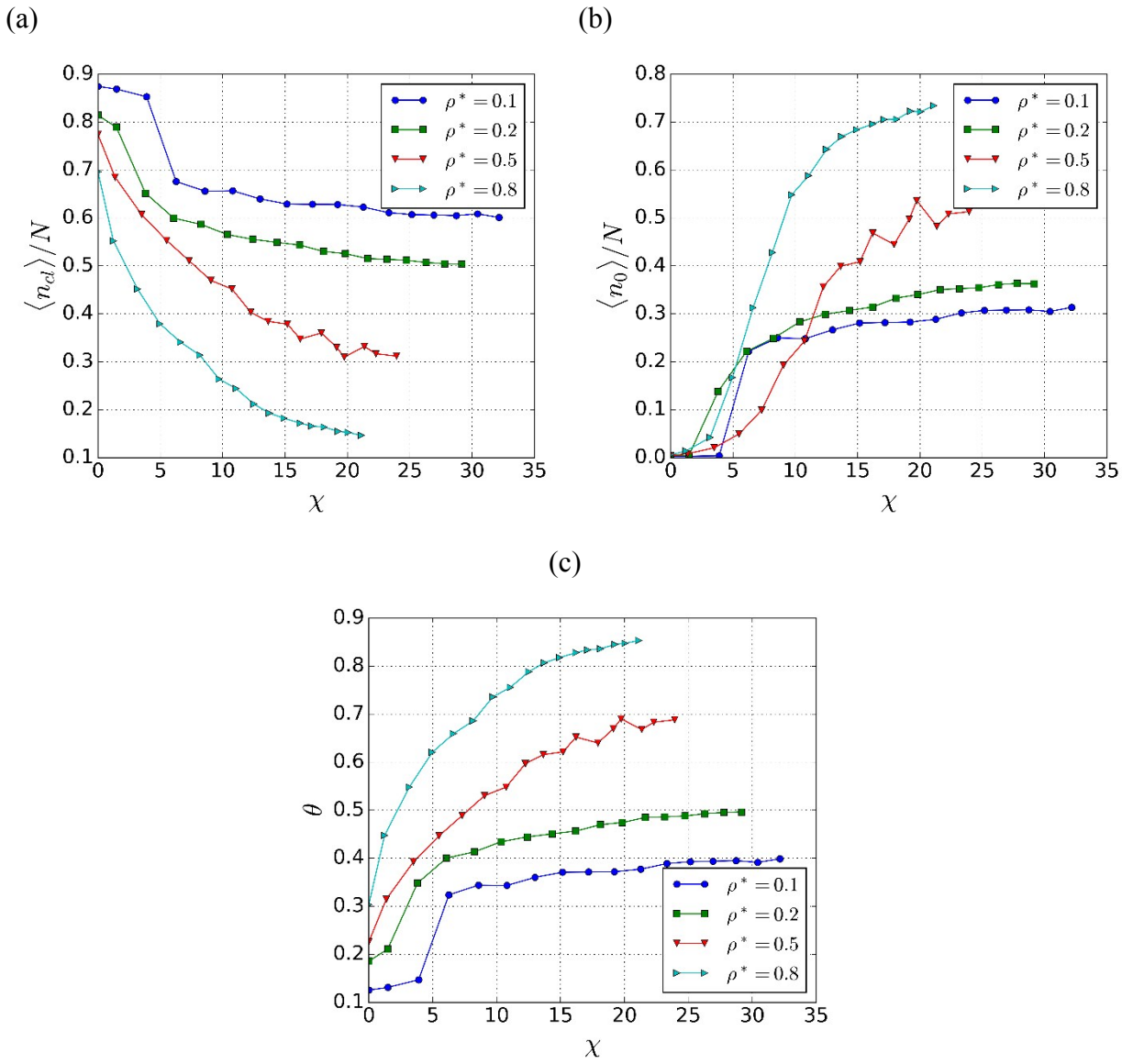

Figure SF8. (color online) (a). Mean number of clusters normalized with total number of particles N. (b). average population of the largest cluster (normalized) (c). clustering parameter θ; all are plotted as a function of the activity parameter χ; for the case of N = 2000.

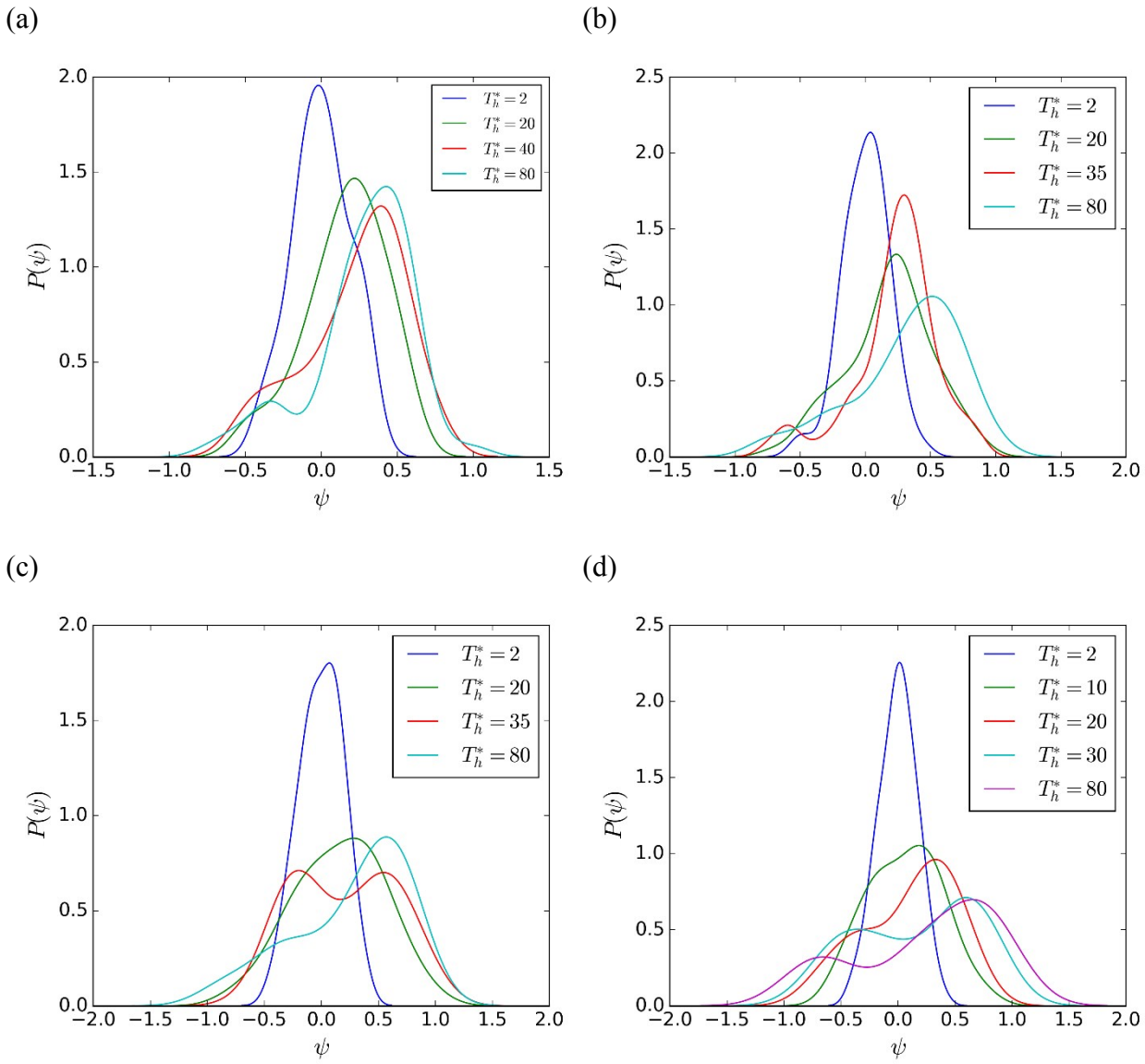

Figure SF9. (color online) Distributions $P(\psi)$, at the respective hot particles' temperature (for N = 2000). (a), (b), (c) and (d) correspond to the systems at the density of $\rho^* = 0.1$, 0.2, 0.5 and 0.8 respectively. The value of χ that corresponds to the value of T^*_h at which $P(\psi)$ develops a bimodal, is referred as the critical activity ratio χ^*. From the figure, we observe that $P(\psi)$ become bimodal at $T^*_h =$ 40, 35, 35 and 30 respectively for $\rho^* = 0.1$, 0.2, 0.5 and 0.8. The corresponding $\chi^* =$ 17.19, 14.33, 12.24 and 9.70 respectively.

(a) (b)

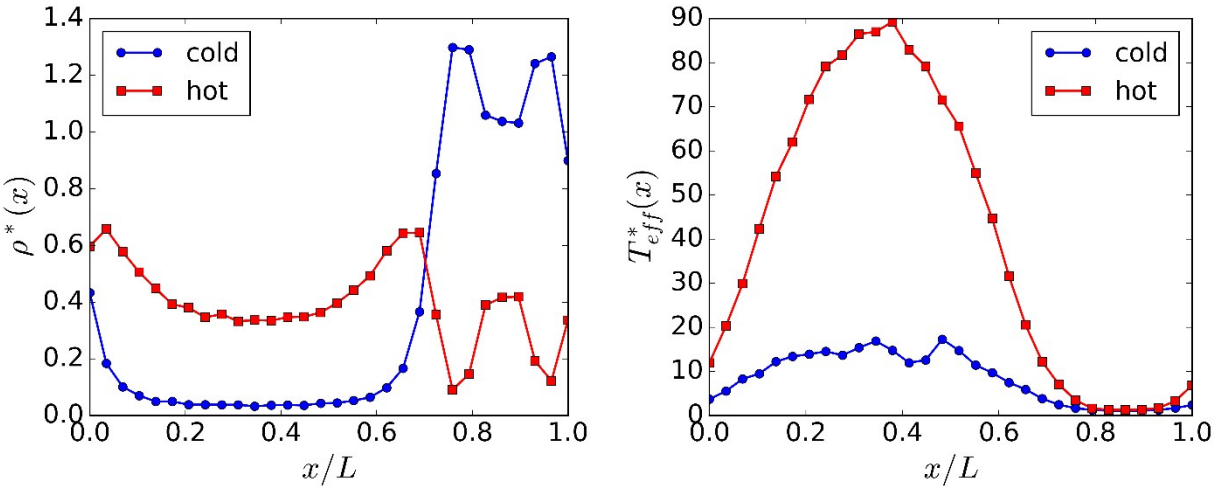

Figure SF10. (color online) Density and effective temperature profiles of the hot and cold particles, depicted in (a) and (b) respectively, for the system with $N = 8000$ and $\rho^* = 0.8$ at the imposed hot particles' temperature $T^*_h = 80$.